Eur. Radiol. 9, 546–551 (1999)

European
Radiology

Original article

Spiral CT angiography of renal arteries: comparison with angiography

G. Wittenberg, W. Kenn, A. Tschammler, J. Sandstede, D. Hahn

Institut für Röntgendiagnostik der Universität Würzburg, Josef-Schneider-Strasse 2, 97080 Würzburg, Germany

Received: 23 June 1997; Revision received: 6 January 1998; Accepted: 29 April 1998

Abstract. A prospective study was carried out to determine the accuracy of spiral CT angiography (CTA) in the detection of renal artery stenosis (RAS). Eighty-two patients with arterial hypertension underwent CTA and digital subtraction angiography (DSA) to exclude RAS. For CTA a contrast medium bolus of 100–150 ml (flow rate 3 ml/s) was injected. A 24 or 40 s CTA was started at the origin of the superior mesenteric artery after a delay time determined by test bolus injection (collimation = 2 mm, pitch = 1/1.5). For stenosis detection transverse images supported by maximum intensity projections (MIP) or multiplanar reconstruction projections were used. Of 197 renal arteries examined (including 33 accessory arteries), 34 RAS were visualized using DSA. With CTA, one hemodynamic RAS was missed and one additional hemodynamic RAS was found. Sensitivity/specificity was calculated to be 94 %/98 %. For hemodynamically relevant RAS (> 50 %) the sensitivity/specificity was 96 %/99 %. CTA additionally depicted five adrenal masses. The high accuracy rate of RAS detection thus allows the use of CTA as a screening method in patients with arterial hypertension to exclude a renovascular cause.

Key words: Hypertension, renal – Renal angiography – Renal arteries, stenosis or obstruction – Computed tomography (CT), helical technology – Computed tomography (CT), three-dimensional

Introduction

Renal artery stenoses (RAS) are in less than 5 % of cases the cause of arterial hypertension; but in these patients angioplasty or vascular surgery may cure RAS-induced hypertension or avoid the need for hemodialysis. Today the method of choice for the detection of RAS is arterial digital subtraction angiography (DSA). Because of the potential risks of invasive DSA it is necessary to search for a noninvasive or less invasive method for detecting RAS with a high diagnostic accuracy. Intravenous DSA and radionuclide scintigraphy have shown insufficient degrees of sensitivity [1, 2] and color-coded duplex sonography depicted in several examination protocols a great range of accuracy rates [3–6].

The introduction of spiral CT has made continuous data acquisition possible in a large patient volume during a single-breath hold. It is therefore possible to visualize vascular structures on the transverse images and also to reconstruct secondary images, such as shaded-surface display (SSD), maximum intensity projections (MIP), and multiplanar reformatting of the vascular system [7–10]. Previous studies have reported a high morphological correlation between the findings of spiral CT angiography (CTA) and DSA, especially for renal arteries [11–18]. Other previous studies have described the optimal CTA parameters and the optimal method of image analysis for detecting arterial stenoses, with a high correlation between the real and measured degree of stenosis [10, 19, 20].

The purpose of this prospective study was to evaluate the accuracy of the CTA in the depiction of RAS in comparison with DSA using our examination and evaluation protocol.

Patients and methods

Patients

To date the renal arteries of 147 patients (71 women, 76 men) have been examined by CTA. In one patient a transplanted kidney was examined. In 82 patients we were able to correlate the results of CTA and DSA. All patients had a history of arterial hypertension and were suspected to have a renal artery stenosis by their attending physician. The mean age of the patients was 51.5 years (range 21–76 years). In all cases the first diag-

Correspondence to: G. Wittenberg

nostic imaging was CTA; initially every patient also underwent DSA. With increasing CTA experience DSA was performed only in patients with renal artery stenosis.

Arterial DSA

DSA (Angiodiagnost 3, Philips, Eindhoven, The Netherlands) was performed by positioning a 5 Fr pigtail catheter just above the renal arteries using a femoral approach. Contrast medium (30 ml of iopromide, 300 mg I/ml; Ultravist 300, Schering, Berlin, Germany) was then injected at a rate of 15 ml/s. Images (2 per second) were obtained in frontal, 15° right and left anterior oblique projections with a field of view of 36 cm. In cases of inadequate visualization of the renal arteries – such as results from overlapping of the superior mesenteric artery or inadequate view of the ostium – selective renal angiography was performed using a 5 Fr cobra catheter. The total volume of injected contrast agent varied between 95 ml and 170 ml.

Spiral CT

At first the CTA was performed using a Somatom plus (SP) scanner ($n = 32$), which has since been replaced by a Somatom plus 4 (SP4) scanner (both scanners by Siemens, Erlangen, Germany) ($n = 115$). The maximum continuous scanning time of the SP/SP4 is 24/40 s; the tube rotation time is 1/0.75 s. The precontrast examinations (collimation 5 mm; pitch 1; reconstruction interval 5 mm) were always started at the top of the first lumbar vertebra covering the kidneys. In these scans the ostium of the superior mesenteric artery – the starting point of the following CTA – was visualized as well as the adrenal glands in order to exclude a mass.

Transit time determination. After locating the renal arteries, 10 ml contrast agent (iopromide, 300 mg I/ml; Ultravist 300, Schering, Berlin, Germany) was manually injected as a fast bolus into a brachial vein. After a delay of 15 s a dynamic sequence of scans (1 s interscan delay, no table incrementation) was started at the level of the renal arteries. The time the contrast medium requires to travel from the brachial vein to the abdominal aorta was estimated as the time interval between the beginning of the injection and the maximum contrast enhancement of the aorta. This transit time was then increased by 5 s because, from our previous experience with CTA, maximum contrast enhancement will be reached later after injecting a larger volume of contrast agent.

Spiral CT angiography. Spiral CT was started at the origin of the superior mesenteric artery. Between 100 and 150 ml contrast agent (iopromide, 300 mg I/ml; Ultravist 300, Schering, Berlin, Germany) was injected using an automatic injector (flow rate 3 ml/s). A collimation of 2 mm, a table speed of 2 mm/s (SP scanner) or 3 mm/s (SP4 scanner) and a reconstruction interval of 1 mm were chosen. The data acquisition of the SP scanner is limited to 24 s. That means that it is limited to an evaluable spiral CT length of 44 mm. The spiral CT length of the SP4 scanner was extended to the iliac arteries. A tube voltage of 120 kV and a tube current of at least 165 mA were chosen in both scanners [19]. During data acquisition patients were asked to hold a deep breath. In all cases CTA was performed first.

Data analysis. At first transverse images were calculated with an interval of 1 mm using the standard algorithm in the SP scanner (360° linear interpolation algorithm) or the kernel AB40 in the SP4 scanner (180° linear interpolation algorithm) [19]. For the evaluation of the renal arteries the transverse images were supported by secondary image reconstructions such as shaded-surface display (SSD) on the SP scanner and maximum intensity projections (MIP) on the SP4 scanner. In cases of extensive arterial wall calcification additional multiplanar reformatted pictures (MRP) were calculated.

For calculation of the SSD a gradient-shaded surface-rendering algorithm integrated in both scanners was used. Before image reconstruction all bone and organ structures that did not belong to the kidneys or their vascular system were edited from the cross-sectional images. The appropriate threshold level (110 up to 220 HU) depended on the degree of contrast enhancement in the arteries. In this method all structures with densities above the selected threshold level were visualized on the three-dimensional images, such as the contrast-enhanced arteries and the mural calcifications. For the evaluation of the renal arteries, the visualization of the anatomic SSD in different unrestricted views was calculated.

Before generating MIP reconstructions the cross-sectional images were also edited to remove osseous structures that could obscure contrast material. In MIP reconstructions, unlike SSD, it is possible to differentiate between vascular lumen perfused with contrast agent and mural calcifications. For the evaluation of the renal arteries, images in postero-anterior, left and right anterior oblique and cephalocaudal views were created. MIP reconstructions were used, in each case examined with the SP4 scanner, for the visualization of RAS and the anatomy. An advantage of MIP reconstructions in comparison with assessment of the transverse images is the easy visualization of craniocaudal-directed stenoses. This rendering technique was not available on the SP scanner.

Multiplanar reformatted images were calculated with interactively defined linear cut lines following the vascular structures. The two-dimensional MRP also allows the differentation between perfused vascular lumen and vascular wall calcifications. MRP were used to detect RAS in calcified renal arteries.

Image analysis. For the detection of RAS the transverse sections were first evaluated. Using the SP scanner SSD supported the analysis in all cases. MRP was used only in patients with excesive arterial wall calcifications.

Using the SP4 scanner, MIP were reconstructed in all patients. MRP were also calculated in patients with arterial wall calcifications for the assessment of the renal arteries. The analysis included an evaluation of the main renal branches and the accessory arteries. The stenoses were graded using a five-point scale: grade 0, < 30 % stenosis; grade 1, 30–49 % stenosis; grade 2, 50–69 % stenosis; grade 3, 70–99 % stenosis; grade 4, occlusion. In patients with RAS arterial wall calcifications, atheromatous deposits in the adjoining aorta or the presence of an aortic aneurysm were noted. Criteria for an optimal CTA of the renal arteries are: (1) continuous contrast enhancement of more than 200 HU in the aorta during the whole data acquisition period and (2) a continuous breath-hold by the patient. If the contrast enhancement in the aorta was less than 100 HU the examination was unacceptable.

A comparative analysis of the two kidneys and the adrenal glands in relation to their size and degree of contrast enhancement was also performed. The average time for creating image recontructions and for film interpretation was 25–35 min.

CTA and DSA were analyzed separately. The CTA reading was done by one observer (CTA experience: 4 years) and the DSA analysis was performed by a different examiner (10 years' experience). The DSA examiner was only informed about the number of the renal arteries seen in CTA before the angiography.

Statistical analysis

The sensitivity and specificity of the results of CTA were calculated in comparison with those of DSA after grading.

Results

In 82 patients 197 renal arteries were visualized including 33 accessory renal arteries (ARA). Thirty of the 33 ARA were shown by CTA and 31 were diagnosed by DSA. In one case the accessory artery was missed because of the short spiral CT length of the SP scanner. In two cases small ARA running behind the inferior vena cava were overlooked. Two ARA were not visualized by DSA in the standard projections because the origin was located just in front of or behind the ostium of the main renal artery; they were interpreted as an early bifurcation. After viewing the CTA results, additional DSA projections, e. g., caudocranial oblique, confirmed the CTA results. In addition to the renal artery visualization, CTA also showed adrenal masses in five patients. In one of the 147 patients the contrast enhancement was below 100 HU, in 32 patients it was 150–200 HU and in 114 patients above 200 HU during the entire scan time.

A degree of stenosis of more than 30 % was described in 35 renal arteries by CTA and in 34 renal arteries by DSA (Table 1). The stenoses were located in the central and peripheral areas of the renal arteries (Fig. 1). In three cases the stenoses were overestimated by CTA; in two of these the estimated degree of stenosis was less than 50 % and in one case less than 70 %. In two cases mural calcification was seen. In these patients DSA had shown only stenoses of less than 30 %.

Table 1. Comparison of the results of digital subtraction angiography (DSA) with those of spiral CT angiography (CTA) of 197 renal arteries in 82 patients

CTA	DSA				
	0–29 %	30–49 %	50–69 %	70–99 %	100 %
0–29 %	160	1		1	
30–49 %	2	9			
50–69 %	1		1		
70–99 %				20	
100 %					2

In two patients the stenoses were underestimated by CTA. In one of these cases a stenosis of less than 50 % was assessed as a stenosis of less than 30 %. With CTA (SP scanner) a high-grade stenosis was overlooked; this stenosis was caused by compression of the renal artery by a small perfused aneurysm (Fig. 2). In this case the false interpretation of the lumen was done using transverse images and three-dimensional SSD. The aneurysm was diagnosed by DSA. After DSA, MRP images were reconstructed. In these images the stenosis could be depicted. In the SP scanner the MIP software was not integrated, and therefore we cannot determine whether it would have been possible to visualize this stenosis in MIP reconstructions. This false negative result was at an early stage of our CTA experience and led to a change in the evaluation protocol.

In our study population a sensitivity of 94.1 %, a specificity of 98.2 % and an accuracy of 97.5 % were calculated for the detection of RAS using CTA. If only hemodynamically relevant stenoses (i. e., stenosis > 50 %) were evaluated, the sensitivity was 95.8 %, the specificity 99.4 % and the accuracy 98.9 %. We noticed no difference between the two scanners as regards RAS visualization, except for the detection of ARA dependent upon the possible CTA length.

Discussion

It is important to detect hemodynamically relevant RAS because of the possibility of treatment for patients with arterial hypertension due to renal artery stenosis, and to prevent renal endstage disease with percutaneous transluminal angioplasty or vascular surgery. Today, the standard for depicting RAS is invasive DSA. Because of its potential risks and the low prevalence of RAS, DSA is not suitable as a screening method. Other examinations, such as captopril scintigraphy and intravenous DSA, have shown inadequate sensitivity or specificity [1, 2]. Color-coded duplex sonography (CCDS), when used on its own, visualized RAS with a sensitivity of 17 % and a specificity of 89 % [3]. Further reports described an increased sensitivity and specificity of up to

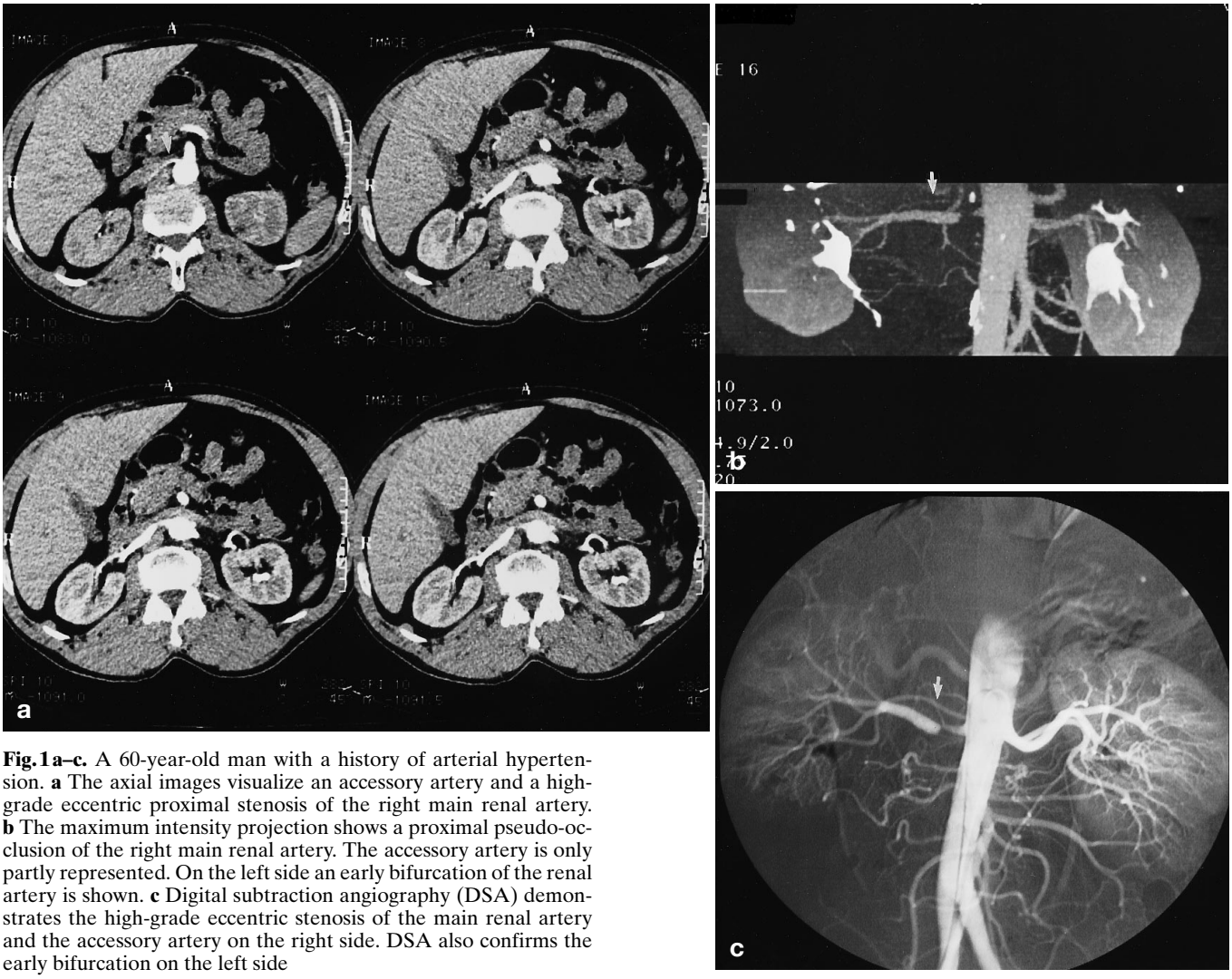

Fig. 1 a–c. A 60-year-old man with a history of arterial hypertension. **a** The axial images visualize an accessory artery and a high-grade eccentric proximal stenosis of the right main renal artery. **b** The maximum intensity projection shows a proximal pseudo-occlusion of the right main renal artery. The accessory artery is only partly represented. On the left side an early bifurcation of the renal artery is shown. **c** Digital subtraction angiography (DSA) demonstrates the high-grade eccentric stenosis of the main renal artery and the accessory artery on the right side. DSA also confirms the early bifurcation on the left side

98 % when indirect signs of stenoses are used, e. g., the resistive index [4–6]. Problems with CCDS are ARA, meteorism, the patient's configuration and cooperation. Experience with magnetic resonance angiography has also shown good results in the detection of RAS, with a sensitivity of up to 100 % and a specificity of up to 95 % [21–24] in the detection of ARA. Previous CTA studies have demonstrated a high morphological correlation with the DSA findings for the visualization of vascular alterations, especially those of the renal arteries. In these studies the sensitivity for the detection of RAS varied between 59 % and 100 % and the specificity between 82 % and 98 % depending upon the examination and the evaluation protocols. The best results are obtained by choosing a collimation of 2 or 3 mm and a table speed of 2–3 mm/s [11–18].

Technical aspects. In vitro studies demonstrated a coherence of the depiction of vascular stenoses and CTA parameters such as collimation, table speed, reconstruction interval and tube current [19, 20]. In both studies the choice of a slice thickness of 2 mm, a maximum pitch of 2 and a reconstruction interval of 1 mm is recommended for the examination of RAS with an expected renal artery diameter between 1 mm and 6 mm. To achieve an acceptable signal-to-noise ratio it is recommended that the tube current is maximized [19]. But the potential tube current is limited by the tube efficiency and is therefore also dependent upon the CTA length and the collimation chosen. For the visualization of most ARA (about 90 %) it is necessary to cover a distance of about 90 mm of the abdominal aorta, suggesting a segment from 20 mm cranial up to 70 mm caudal of the main renal arteries [25]. With the SP scanner we missed one ARA because of the short CTA length. Using the SP4 scanner, covering the distance from the superior mesenteric artery to the iliac arteries, all ARA were visualized, including those that originated in the distal aorta or common iliac artery ($n = 6$). Unfortunately, two small right-sided ARA, running behind the inferior vena cava for a long distance, were depicted only at the second look. Beregi et al. [17] reported that they missed seven of 32 ARA because of the short CTA length. Other authors have described that they visualized all ARA, but in some cases the CTA length was prolonged by a second scan, or an increased colli-

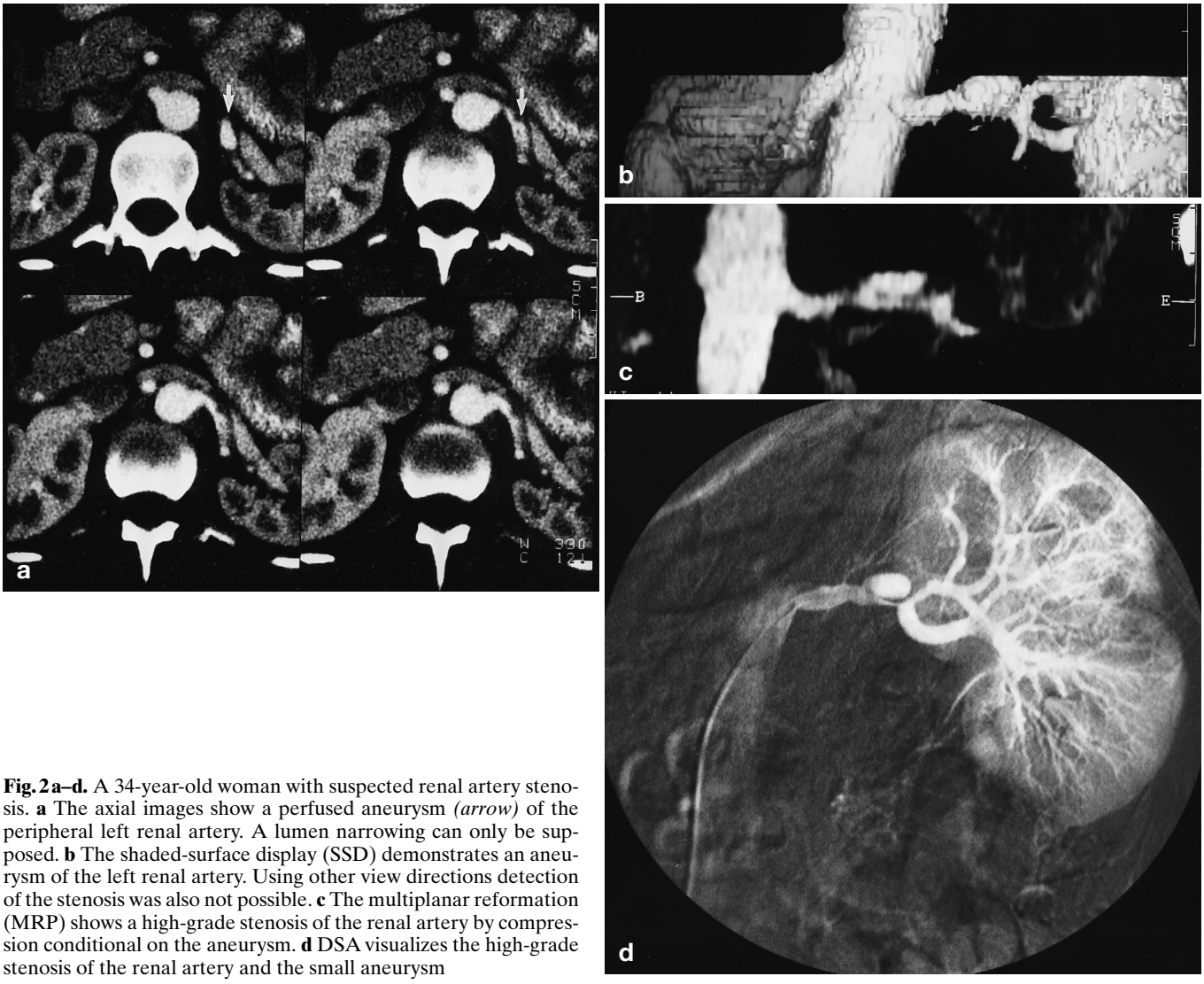

Fig. 2 a–d. A 34-year-old woman with suspected renal artery stenosis. **a** The axial images show a perfused aneurysm *(arrow)* of the peripheral left renal artery. A lumen narrowing can only be supposed. **b** The shaded-surface display (SSD) demonstrates an aneurysm of the left renal artery. Using other view directions detection of the stenosis was also not possible. **c** The multiplanar reformation (MRP) shows a high-grade stenosis of the renal artery by compression conditional on the aneurysm. **d** DSA visualizes the high-grade stenosis of the renal artery and the small aneurysm

mation or an increased table speed was used in patients in whom ARA were suspected [11, 14].

Image quality depends on the contrast enhancement of the renal arteries achieved during the complete scan time. For optimal imaging of the renal arteries data acquisition should begin as soon as contrast enhancement is adequate at the starting point of the CTA, to avoid overlapping of the renal veins. Therefore the transit time has to be determined for each patient individually. During the whole period of data acquisition homogeneous contrast enhancement is necessary. Using an automatic injector with a flow rate of 3 ml/s and a volume of 100–150 ml contrast medium (300 mg I/ml), the opacification was sufficient in 81 of 82 patients. Only in one patient was the contrast enhancement unacceptable (below 100 HU), requiring the examination to be repeated. In our opinion, a high contrast enhancement (> 200 HU) is necessary only for optimal secondary image reconstructions, e. g., MIP or SSD, not for the assessment of the important transverse images. In other reports the volume of contrast agent used varied between 90 and 150 ml and the flow rate varied from 3 to 5 ml/s [11–18].

Stenosis detection. In agreement with previous studies, transverse images are best suited for stenosis detection and assessment of the degree of stenosis. They must be supported, especially in patients with mural calcifications, with MRP and MIP reconstructions. MIP reconstructions should be used because of the similar impression when compared with DSA and the ability to differentiate between perfused arterial lumen and vascular wall calcification. In these cases the SSD technique is not helpful because all structures with a higher density than the chosen threshold are visualized on the reconstructed images and therefore the stenosis assessment is inaccurate. Rubin et al. [14] found that the degree of stenosis in such cases is underestimated using SSD; they also stated that in comparison with DSA the accuracy of the SSD is lower than the accuracy of the MIP reconstructions. Their results also demonstrated that the detection and grading of RAS only by secondary image reconstructions is unacceptable.

Another advantage of CTA is the visualization of the surrounding structures such as thrombotic deposits, aortic aneurysms or the adrenal glands. In our study, five

adrenal masses were diagnosed; Beregi et al. [17] reported that the arterial hypertension in two of his patients was caused by Conn's syndrome. The information on thrombotic deposits, aneurysms and wall calcification may be helpful in deciding whether a radiological or a vascular surgical intervention is preferred. Until now this report has only mentioned the advantages of CTA, but it also has some limitations. One problem with CTA is the visualization of stenoses located in the intrarenal areas of segmental arteries or interlobar arteries. This is still an indication for intra-arterial DSA.

In conclusion, we can say that the less invasive CTA is able to visualize hemodynamically relevant RAS with an accuracy as high as that of DSA. Because of these results, and the low prevalence of RAS, CTA can be recommended as a screening method in patients with arterial hypertension in order to exclude a renovascular cause, with a lower risk than invasive DSA. From the results of with previous studies, we can state that special attention has to be paid to the examination and to the evaluation protocol. We recommend a collimation of 2 mm with a maximum pitch of 1.5 for data acquisition. Image analysis should be performed using transverse images, generally supported by MIP; and in cases with excesive arterial wall calcifications by additional MRP image reconstructions.

References

1. Neufang KFR, Degenhardt S, Moedder U (1987) Diagnostik der renovaskulären Hypertonie mit venöser DSA: Bildqualität und Aussagekraft. Fortschr Röntgenstr 147: 257–261
2. Davidson R, Wilcox CS (1991) Diagnostic usefulness of renal scanning after angiotensin converting enzyme inhibitors. Hypertension 18: 299–303
3. Breitenseher M, Kainberger F, Hubsch P, Trattnig S, Baldt M, Barton P, Karnel F (1992) The screening of renal artery stenoses: the initial results with the value of color Doppler sonography. Fortschr Röntgenstr 156: 228–231
4. Schwerk WB, Restrepo IK, Stellwag M, Klose KJ, Schade-Brittinger C (1994) Renal artery stenosis: grading with image-directed Doppler US. Evaluation of renal resistive index. Radiology 190: 785–790
5. Olin JW, Piedmonte MR, Young JR, DeAnna S, Grubb M, Childs MB (1995) The utility of duplex ultrasound scanning of renal arteries for diagnosing significant renal artery stenosis. Ann Intern Med 122: 833–838
6. Riehl J, Schmitt H, Bongartz D, Bergmann D, Sieberth HG (1997) Renal artery stenosis: evaluation with colour duplex ultrasonography. Nephrol Dial Transplant 12: 1608–1614
7. Kalender WA, Seissler W, Klotz E, Vock P (1990) Spiral volumetric CT with single-breathhold technique, continuous transport and scanner rotation. Radiology 176: 181–183
8. Kalender WA, Vock P, Polacin A, Soucek M (1990) Spiral-CT: eine neue Technik für Volumenaufnahmen. I. Grundlagen und Methodik. Röntgenpraxis 43: 323–330
9. Soucek M, Vock P, Daepp M, Kalender W (1990) Spiral-CT: eine neue Technik für Volumenaufnahmen. II. Klinische Anwendungsmöglichkeiten. Röntgenpraxis 43: 365–375
10. Prokop M, Schaefer C, Kalender WA, Polacin A, Galanski M (1993) Gefäßdarstellungen mit der Spiral-CT. Radiologe 33: 694–704
11. Galanski M, Prokop M, Chavan A, Schaefer CM, Jandeleit K, Nischelsky JE (1993) Renal arterial stenoses: spiral CT angiography. Radiology 189: 185–192
12. Galanski M, Prokop M, Chavan A, Schaefer-Prokop C (1994) CT angiography of the renal arteries. In: Pockieser H, Lechner G (eds) Advances in CT III. Springer, Berlin Heidelberg New York, pp 69–74
13. Galanski M, Prokop M, Chavan A, Schaefer C, Jandeleit K, Olbricht C (1994) Leistungsfähigkeit der CT-Angiographie beim Nachweis von Nierenarterienstenosen. Fortschr Röntgenstr 161: 519–525
14. Rubin GD, Dake MD, Napel S, Jeffrey RB Jr, McDonnell CH, Sommer FG, Wexler L, Williams DM (1994) Spiral CT of renal artery stenosis: comparison of three-dimensional rendering techniques. Radiology 190: 181–189
15. Olbricht CJ, Paul K, Prokop M, Chavan A, Schaefer-Prokop CM, Jandeleit K, Koch KM, Galanski M (1995) Minimally invasive diagnosis of renal artery stenosis by spiral computed tomography angiography. Kidney Int 48: 1332–1337
16. Van Hoe L, Vandermeulen D, Gryspeerdt S, Mertens L, Baert AL, Suetens P, Marchal G, Stockx L (1996) Assessment of accuracy of renal artery stenosis grading in helical CT angiography using maximum intensity projections. Eur Radiol 6: 658–664
17. Beregi JP, Elkohen M, Deklunder G, Artaud D, Coullet JM, Wattinne D (1996) Helical CT angiography compared with arteriography in the detection of renal artery stenosis. AJR 167: 495–501
18. Kaatee R, Beek FJA, De Lange EE, Van Leeuwen MS, Smits HFM, Van der Ven PJG, Beutler JJ, Mali WPTM (1997) Renal artery stenosis: detection and quantification with spiral CT angiography versus optimized digital subtraction angiography. Radiology 205: 121–127
19. Wittenberg G, Schindler R, Trusen A, Schultz G, Jenett M, Kellner M, Tschammler A, Hahn D (1994) Spiral CT: in vitro measurement of stenoses. In: Pockieser H, Lechner G (eds) Advances in CT III. Springer, Berlin Heidelberg New York, pp 129–135
20. Brink JA, Lim JT, Wang G, Heiken JP, Deyoe LA, Vannier MW (1995) Technical optimizatation of spiral CT for depiction of renal artery stenosis: in vitro analysis. Radiology 194: 157–163
21. Fellner C, Strotzer M, Geissler A, Kohler SM, Kraemer BK, Spies V, Held P, Gmeinwieser J (1995) Renal arteries: evaluation with optimized 2D and 3D time of flight MR angiography. Radiology 196: 681–687
22. De Cobelli F, Mellone R, Salvioni M, Vanzulli A, Sironi S, Manunta P, Lanzani C, Bianchi G, Del Maschio A (1996) Renal artery stenosis: value of screening with three-dimensional phase-contrast MR angiography with a phased-array multicoil. Radiology 201: 697–703
23. Silverman JM, Friedman ML, Van Allan RJ (1996) Detection of main renal artery stenosis using phase-contrast cine MR angiography. AJR 166: 1131–1137
24. Wasser MN, Westenberg J, van der Hulst VPM, van Baalen J, van Bockel JH, van Erkel AR, Pattynama PMT (1997) Hemodynamic significance of renal artery stenosis: digital subtraction angiography versus systolically gated three-dimensional phase-contrast MR angiography. Radiology 202: 333–338
25. Boijsen E (1959) Angiographic studies of the anatomy of single and multiple renal arteries. Acta Radiol 183 [Suppl]: 1–99